

Formation of molecules in an expanding Bose-Einstein condensate

V. A. Yurovsky and A. Ben-Reuven

School of Chemistry, Tel Aviv University, 69978 Tel Aviv, Israel

(Received 12 February 2004; published 27 July 2004)

A theoretical analysis of expanding hybrid atom-molecule Bose-Einstein condensates is presented with application to the recent experiments of the Rempe group on ^{87}Rb , in which the formation of ultracold molecules by Feshbach resonance was demonstrated. A mean-field approach is used to describe the molecular association process. The subsequent dissociation of the molecules is treated using a non-mean-field parametric approximation. The latter method is also used to derive optimal conditions for the formation of a molecular condensate.

DOI: 10.1103/PhysRevA.70.013613

PACS number(s): 03.75.Mn, 03.75.Nt, 82.20.Xr

I. INTRODUCTION

Bose-Einstein condensates (BEC's) of homonuclear diatomic molecules have been recently formed in experiments on atomic BEC's [1–4] and on quantum-degenerate Fermi gases [5–9]. These experiments exploited the effect of Feshbach resonance [10], present when the energy of an atomic pair is close to the energy of a bound molecular state. The energy mismatch can be controlled by applying an external magnetic field, thanks to the Zeeman shift created by the difference between the magnetic momenta of the molecule and of the atomic pair. By varying the magnetic field the energy of the molecular state is forced to cross different states of the atomic pairs, belonging to a discrete spectrum in the case of a trapped gas or to a continuum otherwise. The resonance value of the magnetic field strength B_0 corresponds to the crossing of the lowest discrete state or the lower boundary of the continuum, respectively. Most of the experiments were carried out on trapped BEC's, with the exception of [2], in which the varying magnetic field was applied to an expanding BEC.

In the experiments [1–9] the molecules have been formed by sweeping the Zeeman shift through resonance in a backward direction, so that the molecular state crossed the atomic ones downwards. This led to the transfer of population from the lowest atomic state in the case of BEC, or from an energy band in the case of a Fermi gas, to the molecular state, as had been proposed in Ref. [11]. Assuming all the atomic population is initially in the BEC state, the backward sweep would have been ideally suitable for forming molecules, were it not for two destabilizing mechanisms. The resonant molecule is generally populated in an excited rovibrational and electronic state, and therefore can be deactivated by exoergic inelastic collisions with atoms and other molecules (see Refs. [10,12,13]). In addition, during the backward sweep some higher-lying noncondensate atomic states can be populated temporarily. Such quantum transitions, forbidden by semiclassical Landau-Zener-type theories (and called “counterintuitive transitions”—see Ref. [14]), are most notable in strong resonances or at low densities (see Ref. [15]). These two effects restrict the efficiency of conversion from the atomic BEC to the molecular one. The noncondensate atoms produced by molecular dissociation are formed as entangled atomic pairs (see Ref. [15]).

Several theoretical methods are available for the treatment of such processes, in cases in which they cannot be described by standard mean-field (MF) theories. One such method is based on a numerical solution of stochastic differential equations in the positive- P representation, as used in the present context in Refs. [16–18]. Another method is the Hartree-Fock-Bogoliubov formalism (see Ref. [19]), which deals with coupled equations for the atomic $\varphi_a = \langle \hat{\Psi}_a \rangle$ and the molecular $\varphi_m = \langle \hat{\Psi}_m \rangle$ mean fields, describing the condensates, as well as the normal $\langle \hat{\Psi}_a^\dagger \hat{\Psi}_a \rangle$ and the anomalous $\langle \hat{\Psi}_a \hat{\Psi}_a \rangle$ densities. (Here $\hat{\Psi}_a$ and $\hat{\Psi}_m$ are the annihilation operators of the atomic and molecular fields, respectively.) The normal and anomalous densities describe the second-order correlations of the noncondensate atomic fields. These correlations are also taken into account in the microscopic quantum dynamics approach used in Refs. [20–22].

However, the methods used in Refs. [16–22] do not take into account the effects of deactivating collisions. Nevertheless, an appropriate analysis of the formation of molecular BEC's, incorporating all relevant destabilizing effects, requires a non-MF approach into which the damping due to deactivating collisions can be incorporated. Such an approach exists in the form of the parametric approximation (PA) used in Refs. [23–25]. In this case, the momentum representation can be used to write down the atomic annihilation operator $\hat{\Psi}_a(\mathbf{p}, t)$ as

$$\hat{\Psi}_a(\mathbf{p}, t) = \Psi_c(p, t) \hat{\Psi}_a(\mathbf{p}, 0) + \Psi_s(p, t) \hat{\Psi}_a^\dagger(\mathbf{p}, 0), \quad (1)$$

introducing the two c -number functions $\Psi_{c,s}(p, t)$ as coefficients of the creation and annihilation operators at the time $t=0$. This parametric approximation has been generalized in Ref. [15] by allowing for time variation of the molecular field and the deactivating collisions. This formulation becomes mathematically equivalent to the Hartree-Fock-Bogoliubov approach of Ref. [19] when the inelastic collisions are neglected (see Ref. [26]).

In the ^{87}Rb experiments [2], a BEC of about 10^5 atoms has been kept initially in a harmonic trap with frequencies $2\pi \times (50, 120, 170)$ Hz. The magnetic field ramp was started after a preliminary expansion interval $t_p \geq 2$ ms, following the switching off of the trap. This measure leads to a reduc-

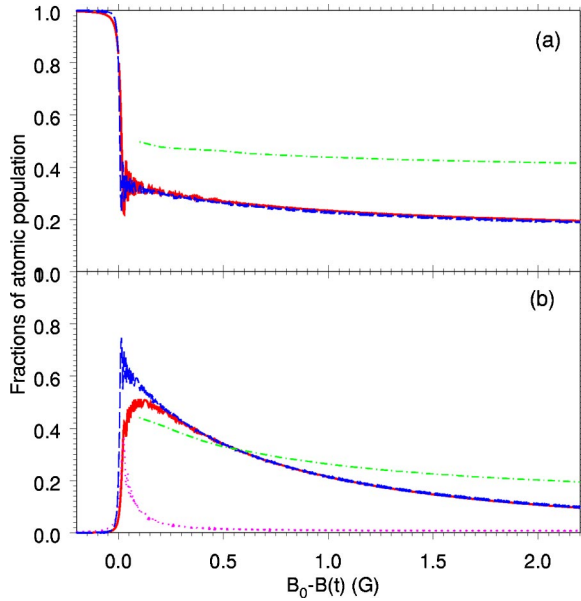


FIG. 1. (Color online) Fraction of atomic population surviving in the atom BEC (a) and converted to molecules (b), calculated using the PA (solid lines) and the MF (dashed lines) approaches for a homogeneous gas with an initial atomic density $3 \times 10^{13} \text{ cm}^{-3}$ and a magnetic ramp speed of 1 G/ms. The fraction of noncondensate atoms calculated with the PA is represented by the dotted line in part (b). The dot-dashed lines represent the fraction of surviving and converted population calculated using the MF approach while taking account of spatial inhomogeneity and expansion.

tion of condensate density and thus improves the conversion efficiency (see Ref. [15]). The field has been ramped from 1008 G to 1005.2 G with various speeds, passing the 1007.4-G resonance of strength $\Delta \approx 0.2$ G (see Ref. [27]) and held for 3 ms. During this time a gradient magnetic field has been applied, leading to a relative motion of the atoms in respect to the molecules, due to the difference of magnetic momenta between a molecule and an atomic pair, $\mu \approx 2.8\mu_B$ (see Ref. [28]). Next, the magnetic field was ramped up to 1008 G (in a forward sweep), converting the molecules back to atoms. The reconverted atoms inherit the velocity of the molecules and thus form a separate condensate cloud.

Comparative analysis shows that non-MF effects are essential to the analysis of molecular dissociation—more so in forward sweeps than in backward ones. Nevertheless, for most aspects of the association stage, an MF approach will suffice in the case of rubidium studied here. Such an MF approach is described in [12,13] (which—contrary to [15]—can be readily extended to traps with inhomogeneity). This statement will be backed by numerical comparisons described at the beginning of Sec. II below and illustrated by Fig. 1.

The analysis of the association stage, using the MF approach, is described in Sec. II below. In Sec. III the dissociation stage is described, using the PA approach. In Sec. IV, optimal conditions for obtaining a molecular BEC in the association stage are investigated. The latter exploration, too, is better carried out using the PA approach.

II. ASSOCIATION OF ATOMS IN AN EXPANDING BEC

The analysis of experiments on expanding condensates must take into account the effects of spatial inhomogeneity. Attempts to extend the PA method in order to incorporate inhomogeneity are very complicated tasks, requiring a huge amount of numerical work. Fortunately, in the case of ^{87}Rb , using a rather weak Feshbach resonance, the analysis can be satisfactorily carried out by using the simpler MF approach. This is demonstrated by a comparison of the numerical results, illustrated in Fig. 1, comparing the atomic and molecular densities calculated with the PA approach of [15] to those calculated with the MF approach of [12,13], under the appropriate conditions. The initial atomic density used corresponds to the peak density reached at the expansion time of 2.3 ms. The values used for the deactivation rate coefficients are $k_a = 7 \times 10^{-11} \text{ cm}^3/\text{s}$ (see Ref. [29]) and $k_m = 5 \times 10^{-11} \text{ cm}^3/\text{s}$ for atom-molecule and molecule-molecule collisions, respectively. The elastic scattering length is $a_a = 99$ atomic units (see Ref. [28]). As one can see, already when the magnetic field is just 0.3 G below the resonance (in a sweep totaling 2.2 G), the results of the two kinds of calculations coincide. In order to understand why they do, one should notice the vanishingly small temporary population of noncondensate atom states, the occupation of which involves an essentially non-MF process. When faster magnetic sweeps or higher densities are considered, the results of the two approaches converge even faster.

The extension of the MF approach of Refs. [12,13] to inhomogeneous expanding gases, including both the trapping and the expansion stages, requires the solution of two coupled Gross-Pitaevskii equations for the atomic $\varphi_a(\mathbf{r}, t)$ and the molecular $\varphi_m(\mathbf{r}, t)$ mean fields:

$$\begin{aligned}
 i\hbar\dot{\varphi}_a(\mathbf{r}, t) &= \left[-\frac{\hbar^2}{2m}\nabla^2 + \epsilon_a(t) + V_a(\mathbf{r}, t) - \frac{i}{2}k_a|\varphi_m(\mathbf{r}, t)|^2 \right. \\
 &\quad \left. + \frac{4\pi\hbar^2}{m}a_a|\varphi_a(\mathbf{r}, t)|^2 \right] \varphi_a(\mathbf{r}, t) + 2g^*\varphi_a^*(\mathbf{r}, t)\varphi_m(\mathbf{r}, t), \\
 i\hbar\dot{\varphi}_m(\mathbf{r}, t) &= \left[-\frac{\hbar^2}{4m}\nabla^2 - \frac{i}{2}k_a|\varphi_a(\mathbf{r}, t)|^2 \right. \\
 &\quad \left. - ik_m|\varphi_m(\mathbf{r}, t)|^2 \right] \varphi_m(\mathbf{r}, t) + g\varphi_a^2(\mathbf{r}, t). \quad (2)
 \end{aligned}$$

Here m is the mass of the atom and $\epsilon_a(t) = -\frac{1}{2}\mu(B(t) - B_0)$ is the time-dependent Zeeman shift of the atom relative to half the energy of the molecular state. The external magnetic field $B(t)$ is kept constant while $t < t_0$ and is linearly ramped at $t > t_0$, letting the resonance be crossed at $t=0$ so that $B(0) = B_0$. The atoms are considered trapped in a harmonic potential

$$V_a(\mathbf{r}, t) = \frac{m}{2} \sum_{j=1}^3 \omega_j^2 r_j^2 \theta(t_0 - t_p - t),$$

which is switched off before the ramping, at $t = t_0 - t_p$. The atom-molecule coupling is related to the phenomenological resonance strength Δ as $|g|^2 = 2\pi\hbar^2|a_a|\mu\Delta/m$ (see Ref. [13]).

The molecular trap potential and elastic collisions involving molecules can be neglected since the molecules are formed after the expansion starts when the trap is switched off and the densities decrease substantially.

The expansion of a pure atomic condensate cloud has been considered in Refs. [30,31]. We generalize this theory here to the case of a hybrid atom-molecule condensate. Let us consider an initial atomic field with a Thomas-Fermi distribution and a zero molecular field at $t < t_0 - t_p$. We can represent the two mean fields in the form

$$\begin{aligned}\varphi_a(\mathbf{r}, t) &= A(t)\Phi_a(\boldsymbol{\rho}, t)e^{iS}, \\ \varphi_m(\mathbf{r}, t) &= A(t)\Phi_m(\boldsymbol{\rho}, t)e^{2iS},\end{aligned}\quad (3)$$

using the scaled coordinates $\rho_j = r_j/b_j(t)$, $1 \leq j \leq 3$, and a scaling factor $A(t) = [b_1(t)b_2(t)b_3(t)]^{-1/2}$. The scales b_j obey the set of equations

$$\ddot{b}_j(t) = \omega_j^2 A^2(t)/b_j(t), \quad b_j(t_0 - t_p) = 1. \quad (4)$$

The phase in Eq. (3),

$$S(t) = \frac{m}{\hbar} \sum_{j=1}^3 r_j^2 \frac{\dot{b}_j(t)}{2b_j(t)} - \frac{\epsilon_0}{\hbar} \int_{t_0 - t_p}^t dt' A^2(t'), \quad (5)$$

accumulates most of the contributions of the kinetic energy. (Here $\epsilon_0 = 4\pi\hbar^2 a_a n_0/m$ is a chemical potential of the atomic BEC and n_0 is its peak density while the trap is on.) As has been shown in Refs. [30,31], the residual kinetic energy terms can be neglected in the Thomas-Fermi regime when the kinetic energy in the initial state (while the trap is on) is negligible compared to ϵ_0 .

Substitution of Eq. (3) into Eq. (2) leads to the following set of coupled equations for the transformed mean fields:

$$\begin{aligned}i\hbar\dot{\Phi}_a(\boldsymbol{\rho}, t) &= \left[\epsilon_a(t) - \frac{i}{2}A^2(t)k_a|\Phi_m(\boldsymbol{\rho}, t)|^2 \right] \Phi_a(\boldsymbol{\rho}, t) \\ &\quad + 2A(t)g^* \Phi_a^*(\boldsymbol{\rho}, t)\Phi_m(\boldsymbol{\rho}, t), \\ i\hbar\dot{\Phi}_m(\boldsymbol{\rho}, t) &= -iA^2(t) \left[\frac{1}{2}k_a|\Phi_a(\boldsymbol{\rho}, t)|^2 + k_m|\Phi_m(\boldsymbol{\rho}, t)|^2 \right] \Phi_m(\boldsymbol{\rho}, t) \\ &\quad + A(t)g\Phi_a^2(\boldsymbol{\rho}, t).\end{aligned}\quad (6)$$

The loss processes and atom-molecule transitions distort $\Phi_a(\boldsymbol{\rho}, t)$ and $\Phi_m(\boldsymbol{\rho}, t)$ from the Thomas-Fermi shapes, leading to additional energy shifts compared to the pure atomic case. These shifts, however, are of the order of $A^2(t)\epsilon_0$ and can only lead to a negligible small shift of the resonance (of less than 10^{-4} G in the present case).

Equations (6) have a rather clear physical sense. They describe a ballistic expansion of the atomic and molecular BEC with the same velocity distribution, reducing the densities by the factor $A^2(t)$ and leading to a rescaling of the coupling and deactivation parameters. This reflects the fact that the acceleration predates the formation of molecules that inherit the velocity of the atoms they are formed from.

The results of a numerical solution of Eq. (6) are shown in Fig. 1. The inhomogeneity and the expansion reduce the atomic density, leading to a slower loss of atoms and mol-

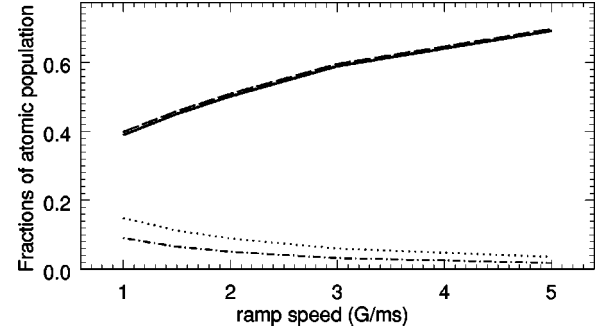


FIG. 2. Fraction of atomic population surviving in the atomic condensate (solid line) and that converted to molecules (dot-dashed line) calculated with the MF approach, taking account of spatial inhomogeneity and expansion, are shown for $k_a = 10^{-10}$ cm³/s. The dashed and dotted lines show the fraction of surviving and converted populations, respectively, calculated for $k_a = 7 \times 10^{-11}$ cm³/s.

ecules. The dependence on the sweep rate is presented in Fig. 2 for two values of k_a (the best fit and upper limit taken from Ref. [29]). The results are in agreement with the experimental data of Ref. [2] reporting that $\sim 7\%$ of atoms are converted to molecules and $\sim 30\%$ remain in the atomic BEC for ramp speeds less than 2 G/ms.

III. DISSOCIATION OF MOLECULES ON A FORWARD SWEEP

Consider now the dissociation of molecules on a forward sweep, when the molecular state crosses the atomic ones upwards. Such a sweep has been used in experiments for detection of molecules. The experiments demonstrate no significant dependence of the reconversion efficiency on the ramp speed. Our calculations using the PA demonstrate that under the experimental conditions all molecules are dissociated except for a small part lost due to deactivating collisions during the sweep. The molecules dissociate to entangled atomic pairs in a wide energy spectrum (see Ref. [15]) characterized by the peak energy E_{peak} . The calculations demonstrate that E_{peak} increases with the ramp speed (see Fig. 3). The results show no significant dependence on the molecular density, justifying the applicability of the homogeneous den-

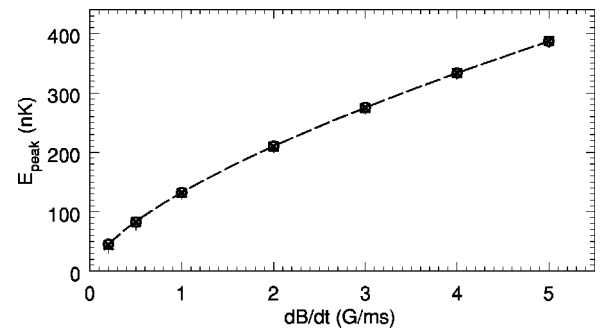


FIG. 3. Peak energy of the noncondensate atoms formed by the dissociation of molecules in a forward sweep, calculated using Eq. (8) (solid line) and the PA, for the initial molecular densities 10^{10} (\circ), 10^{11} (\times), and 10^{12} ($+$) cm⁻³.

sity approximation to real inhomogeneous situations.

In the present case the dissociation can be described by a simple analytical curve-crossing model based on the approach of Ref. [13]. A molecule dissociates into two entangled atoms, each with an energy E , by a crossing occurring at $\mu(B(t)-B_0)=2E$. In the weak-resonance case, the quantum curve-crossing theory [25] and the semiclassical Landau-Zener theory yield approximately the same result for the crossing probability—i.e., $e^{2\pi\lambda}-1 \approx 1-e^{-2\pi\lambda} \approx 2\pi\lambda$, where $\lambda=8\pi\hbar a_n m(t)\Delta/(m|\dot{B}|)$ (see Ref. [15]). Neglecting deactivating collisions the molecular density $n_m(t)=|\varphi_m(t)|^2$ is given by the solution of Eq. (50) in Ref. [13]:

$$n_m(t) = n_m(t_d) \exp \left[-2 \frac{a_a \mu \Delta}{\hbar^2} \int_{t_d}^t dt' \sqrt{m \mu [B(t') - B_0]} \right],$$

where t_d is the starting time of the dissociation ramp. The resulting energy distribution of the produced atoms is given by

$$f(E) = \frac{1}{2} \sqrt{E} E_{\text{peak}}^{-3/2} \exp \left[-\frac{1}{3} (E/E_{\text{peak}})^{3/2} \right], \quad (7)$$

with

$$E_{\text{peak}} = \frac{1}{2m} \left(\frac{\hbar^2 m |\dot{B}|}{4a_a \Delta} \right)^{2/3}. \quad (8)$$

This model is in good agreement with the numerical results (see Fig. 3). Similar models have been independently developed in Refs. [4,22]. Recent measurement of the dissociation energy reported in Ref. [32] are in excellent agreement to these models.

IV. OPTIMIZED MOLECULAR FORMATION ON A BACKWARD SWEEP

Figure 1 demonstrates that the molecular population reaches a maximum, corresponding to a conversion efficiency $\sim 50\%$, about 0.1 G below the resonance, and falls by half about 0.5 G below the resonance. The low conversion efficiency observed in experiments [2] is due to collision loss during the long sweep to 2.2 G below the resonance. Although the PA results of Fig. 1 overestimate the loss by neglecting the expansion, the molecular population of the expanding gas falls by half on reaching 2.2 G. Under the conditions of the experiments the lifetime of the molecules formed is about 0.5 ms, too short for an effective detection. As in the case of Na (see [15]), the lifetime and conversion efficiency increase on reducing the initial condensate density. This is demonstrated in Fig. 4, showing the results of calculations using the PA [15] for the homogeneous case. The use of this non-MF approach is important for such situations, as the MF approach becomes inadequate in the vicinity of the peak molecular occupation (see Fig. 1) and at low condensate densities. A use of the weaker resonance at 685 G with $\Delta \approx 17$ mG $\mu=14\mu_B$ (see Ref. [28]) should increase the conversion efficiency (see Fig. 4).

As in the case of Na studied in Ref. [15], the conversion efficiency is determined by a concurrence of three processes:

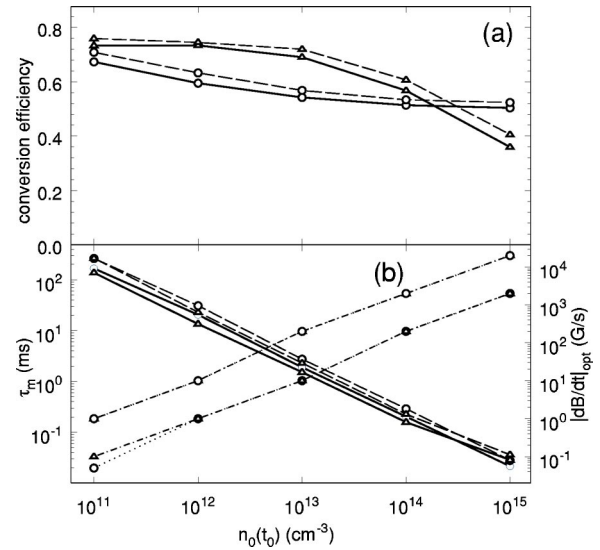


FIG. 4. Conversion efficiency (a) and lifetime of the molecular BEC τ_m (b) at the optimal ramp speed $(dB/dt)_{\text{opt}}$, all plotted as functions of the initial atomic density n_0 , calculated with the homogeneous PA, for the resonances at 1007 G (circles) and 685 G (triangles), using two rates of molecule-molecule deactivation, 10^{-10} cm $^{-3}$ /s (solid lines) and 0.5×10^{-10} cm $^{-3}$ /s (dashed lines). The dash-dotted and dotted lines in part (b) plot $(dB/dt)_{\text{opt}}$ for the same two rates, respectively.

the association of the atomic BEC and the two loss processes — the dissociation of the molecular BEC onto noncondensate atoms and the deactivation by inelastic collisions. A reduction of the ramp speed enhances all three processes. The calculations of Ref. [22], taking no account of the inelastic collisions, result in a monotonic increase of the conversion efficiency with a decrease of the ramp speed (see also Fig. 5). The inelastic collisions, however, tend to reduce the conversion efficiency at slow ramp speeds (see Fig. 5), as has also been demonstrated in Ref. [15]. The optimal ramp speed increases with the density and the resonance strength (see Fig. 4).

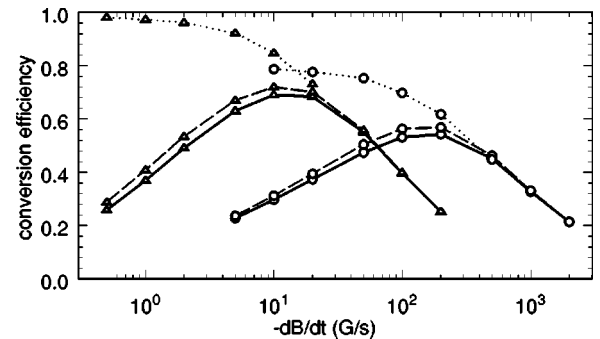


FIG. 5. Conversion efficiency as a function of the ramp speed dB/dt , calculated with the homogeneous PA, given an initial atomic density of 10^{13} cm $^{-3}$ for the resonances at 1007 G (circles) and 685 G (triangles), using the rates of molecule-molecule deactivation $k_m=10^{-10}$ cm $^{-3}$ /s (solid lines) and $k_m=10^{-10}$ cm $^{-3}$ /s (dashed lines). The dotted lines demonstrate the results of calculations taking no account of inelastic collisions (i.e., $k_a=k_m=0$).

V. CONCLUSIONS

The experiments [2] on the formation of molecules from a ^{87}Rb BEC due to a Feshbach resonance, using a backward sweep, are sufficiently described by a MF theory of expanding atom-molecule BEC's, obtaining good agreement with the experimental data. Non-MF calculations, using the PA

method, produce the energy spectrum of entangled noncondensate atom pairs formed by molecular dissociation in a forward sweep, following the association. Analysis of optimal conditions for the formation of a molecular BEC in a backward sweep shows the existence of an optimal ramp speed, depending on the resonance strength and on the initial gas density.

-
- [1] J. Herbig *et al.*, *Science* **301**, 1510 (2003).
 [2] S. Dürr, T. Volz, A. Marte, and G. Rempe, *Phys. Rev. Lett.* **92**, 020406 (2004).
 [3] K. Xu *et al.*, *Phys. Rev. Lett.* **91**, 210402 (2003).
 [4] T. Mukaiyama *et al.*, *Phys. Rev. Lett.* **92**, 180402 (2004).
 [5] C. A. Regal, C. Ticknor, J. L. Bohn, and D. S. Jin, *Nature (London)* **424**, 47 (2003).
 [6] K. E. Strecker, G. B. Partridge, and R. G. Hulet, *Phys. Rev. Lett.* **91**, 080406 (2003).
 [7] J. Cubizolles *et al.*, *Phys. Rev. Lett.* **91**, 240401 (2003).
 [8] S. Jochim *et al.*, *Phys. Rev. Lett.* **91**, 240402 (2003).
 [9] M. W. Zwierlein *et al.*, *Phys. Rev. Lett.* **91**, 250401 (2003).
 [10] E. Timmermans, P. Tommasini, M. Hussein, and A. Kerman, *Phys. Rep.* **315**, 199 (1999).
 [11] F. H. Mies, E. Tiesinga, and P. S. Julienne, *Phys. Rev. A* **61**, 022721 (2000).
 [12] V. A. Yurovsky, A. Ben-Reuven, P. S. Julienne, and C. J. Williams, *Phys. Rev. A* **60**, R765 (1999).
 [13] V. A. Yurovsky, A. Ben-Reuven, P. S. Julienne, and C. J. Williams, *Phys. Rev. A* **62**, 043605 (2000).
 [14] V. A. Yurovsky, A. Ben-Reuven, P. S. Julienne, and Y. B. Band, *J. Phys. B* **32**, 1845 (1999); V. A. Yurovsky and A. Ben-Reuven, *Phys. Rev. A* **63**, 043404 (2001).
 [15] V. A. Yurovsky and A. Ben-Reuven, *Phys. Rev. A* **67**, 043611 (2003).
 [16] U. V. Poulsen and K. Mølmer, *Phys. Rev. A* **63**, 023604 (2001).
 [17] J. J. Hope, M. K. Olsen, and L. I. Plimak, *Phys. Rev. A* **63**, 043603 (2001); J. J. Hope, *ibid.* **64**, 053608 (2001); J. J. Hope and M. K. Olsen, *Phys. Rev. Lett.* **86**, 3220 (2001).
 [18] K. V. Kheruntsyan and P. Drammond, *Phys. Rev. A* **66**, 031602 (R) (2002).
 [19] M. Holland, J. Park, and R. Walser, *Phys. Rev. Lett.* **86**, 1915 (2001).
 [20] T. Köhler and K. Burnett, *Phys. Rev. A* **65**, 033601 (2002).
 [21] T. Köhler, T. Gasenzer, and K. Burnett, *Phys. Rev. A* **67**, 013601 (2003).
 [22] K. Góral *et al.*, e-print cond-mat/0312178.
 [23] A. Vardi, V. A. Yurovsky, and J. R. Anglin, *Phys. Rev. A* **64**, 063611 (2001).
 [24] V. A. Yurovsky, *Phys. Rev. A* **65**, 033605 (2002).
 [25] V. A. Yurovsky, A. Ben-Reuven, and P. S. Julienne, *Phys. Rev. A* **65**, 043607 (2002).
 [26] V. A. Yurovsky and A. Ben-Reuven, *J. Phys. B* **36**, L335 (2003).
 [27] T. Volz *et al.*, *Phys. Rev. A* **68**, 010702 (R) (2003).
 [28] A. Marte *et al.*, *Phys. Rev. Lett.* **89**, 283202 (2002).
 [29] V. A. Yurovsky and A. Ben-Reuven, *Phys. Rev. A* **67**, 050701 (R) (2003).
 [30] Yu. Kagan, E. L. Surkov, and G. V. Shlyapnikov, *Phys. Rev. A* **54**, R1753 (1996).
 [31] Y. Castin and R. Dum, *Phys. Rev. Lett.* **77**, 5315 (1996).
 [32] S. Dürr, T. Volz, A. Marte, and G. Rempe, e-print cond-mat/0405606.